Accuracy of water vapor permeability of building materials reassessed by measuring cup's inner relative humidity

T. Colinart, P. Glouannec

Version of Record: https://www.sciencedirect.com/science/article/pii/S0360132322002797
Manuscript_16af24b67d61389aa182f5ba0ce06133

Accuracy of water vapor permeability of building materials reassessed by measuring cup's inner relative humidity

T. COLINART[1*], P. GLOUANNEC[1]

[1] Univ Bretagne Sud, UMR CNRS 6027, IRDL, 56100 Lorient, France

Corresponding author:

Thibaut COLINART

IRDL – Université de Bretagne Sud

Rue de saint Maudé, BP 92116,

56321 Lorient Cedex, France

Phone: 33/0 2 97 87 45 17

Fax: 33/0 2 97 87 45 72

Mail : thibaut.colinart@univ-ubs.fr

Abstract

Cup experiments are the most widely used method to measure the water vapor permeability of porous building materials. For this test, cup assembly is designed to create a vapor pressure gradient across a sample and, thus, to allow vapor diffusion through it. Water vapor permeability is assessed by weighing cup assembly over time. While the external conditions are generally well controlled, appropriate solid desiccants or saturated salt solutions are used to control the conditions inside the cup. However, precise knowledge of these conditions is crucial, as they are used to calculate permeance and hence water vapor permeability. In this study, dry and wet cup experiments were performed with different solid desiccants or saturated salt solutions on nine materials with Sd-values ranging from 0.08 m to more than 1 m. In all the experiments, the relative humidity within the air layer in the cup was measured with wireless sensors. The results showed that relative humidity was rarely the same as the expected value and that the relative humidity of solid desiccant also varied over time, resulting in from 5 % to 450 % relative errors in the predicted Sd-value. A correction method is proposed to assess the "real" Sd-value from the theoretical Sd-value and differences between dry and wet cup experiments are discussed.

Keywords

Cup method; Sd-value; relative humidity; surface film resistance; porous building materials.

Highlights

- Dry and wet cup experiments on nine materials with different permeability.
- Tests performed with solid desiccants or saturated salt solutions.
- Relative humidity measured within the air layer in the cup with a wireless sensor.
- Measured RH differed from the expected value and may also vary over time.
- Relative errors in the predicted Sd-value ranged between 5 % and 450 %.

1 Introduction

Water vapor permeability (and related properties: water vapor diffusion resistance factor or Sd-value) of a building material is a property describing the ability of water vapor to pass through a material by diffusion. This property needs to be known to design an airtight and moisture proof building envelope. For instance, the French standard on timber frame building envelope [1] requires a minimum exterior to interior Sd-value ratio of 1:5 to ensure that moisture can diffuse to the outside. The risk of interstitial condensation due to water vapor diffusion in other building envelopes can be evaluated according to ISO 13788 [2]. For instance, this method has been applied when retrofitting walls with internal thermal insulation [3]. The Sd-value of a vapor barrier should normally be set to prevent moisture ingress into the insulation layer during wintertime. However, since this vapor barrier may limit the drying out of the masonry wall towards the inside of the building during summertime [4], diffusion-open capillary active systems whose drying potential depends -among others- on the Sd-value, have been the subject of increasing interest [5]. Besides, stochastics studies have reported that the hygrothermal behavior of the building envelope may depend on the accuracy of input parameters, including the water vapor diffusion resistance factor [6], meaning this property has to be measured precisely.

Among the most common measurement methods (sweat guarded hot plates [7], permeation cells [8], or inverse methods applied to diffusion experiments [9,10]), the cup method [11-13] remains the most widely used thanks to its simplicity. Broadly, this test consists in measuring the moisture flow due to relative humidity gradient across a sample sealed on a cup containing desiccant or saturated salt solution under steady state and isothermal condition. Despite the good repeatability and reproducibility of this test performed in one lab [14], several round robin tests showed inter-laboratory discrepancies ranging from

8 % to 450 % whatever the vapor-tightness of the materials [15-19]. There are three main reasons for these differences [20].

The first concerns the experimental design, *e.g.* how the sample is assembled with the cup. Examples of test assembly are proposed in the standards [11-13], but some may create a "masked edge" that needs to be corrected (even if its influence on the results is limited [18,21]). Attention also needs to be paid to sealing [22-24] as leakage through the sealed edge leads to overestimation of permeability [18], particularly for vapor-tight materials, while penetration of molten sealants into porous materials may reduce the effective area [11].

The second reason concerns the importance of surface air resistances compared to the material water vapor resistance. One surface resistance is due to vapor diffusion across still air layer in the cup. Even if the air layer thickness should be 15 ± 5 mm thick to limit its influence [11], it should nevertheless be taken into account in the analysis, particularly in the case of vapor permeable materials [21]. Two methods are proposed in ISO 12572 [11] to evaluate this resistance: using Schirmer formula (Appendix G) or testing two samples of different thicknesses (Appendix H). However, the results of the two methods can differ by a factor of 4 [25,26]. Another type of surface resistance is due to convection above the cup. Even if the air velocity above the samples should be at least 2 $m \cdot s^{-1}$ to limit its influence [11], this recommendation is in fact solely respected and convective surface air resistance should be evaluated as a function of air velocity (as in [27]) to be included in the analysis. However, even when this resistance is taken into consideration, previous studies have shown that the water vapor resistance of material can decrease significantly with increasing velocity [16,25,28].

The third reason concerns adequate control of ambient conditions. Barometric pressure, temperature, and relative humidity outside the cup do not vary much during experiments, so that their influence on water vapor permeability is expected to be limited [29,30], whereas

relative humidity inside the cup remains unknown. For dry cup experiments, desiccants like Silica Gel [18,30,31], Calcium Chloride $CaCl_2$ [15,17,18,32-34], or Magnesium Perchlorate $Mg(ClO_4)_2$ [18] are recommended to ensure 0 %RH within the cup. However, this theoretical value does not seem to be reached as highlighted by measured relative humidity values ranging between 3 %RH and 17 %RH inside the cup at the onset of the test [35-37]. A previous study performed on wood fiber insulation showed that using measured relative humidity in the analysis may result in up to 300 % difference in the water vapor diffusion resistance factor compared to theoretical calculations [37]. Moreover, as moisture flows into the cup, the desiccant is progressively saturated (*i.e.* its absorptive power decreases), relative humidity within the cup increases over time (*i.e.* the difference in vapor pressure decreases) and the density of the water vapor flow rate decreases [34,35,37]. For instance, the increase in relative humidity in permeable materials was shown to range between 7 %RH and 10 %RH over 24h [35,37], which prevented the steady state from being reached. To take measurements under different relative humidity values (like in wet cup experiments), saturated salt solutions are used. Nevertheless, the theoretical relative humidity inside the cup is evaluated at equilibrium, whereas non-equilibrium prevails during the experiments.

Exact knowledge of the relative humidity within the air layer is thus crucial for cup experiments. Previous works [33,38] measured it without showing the variations. In the present study, we measured the relative humidity within the air layer, and then evaluated the true permeability of nine building materials, using desiccants, and saturated salt solutions.

2 Materials and Methods

2.1 Materials

Nine building materials used in previous works [37,39-42] were tested: wood fiber insulation (WFI), gypsum board (Gyp.), two samples of Aerated Autoclaved Concrete (AACa & AACb), two samples of OSB/3 (OSBa & OSBb), hollow concrete blocks (HCB), rainscreen membrane (Memb.) and hemp concrete (HC). All the samples have surface of 100 x 100 mm. Their thickness d and dry density ρ are listed in Table 1. All the materials cover a wide range of permeability.

Material		d [mm]	ρ [kg·m^{-3}]	Sd [m] (declared/literature)		
				dry	wet	
Insulation	WFI	40	50	0.08 (decl.)		Highly permeable materials
	AACa	20.4	604	0.2 [43]	0.06 [43]	
	AACb	18.9	524	0.2 [43]	0.06 [43]	
	HC	50.4	330	0.3 [42]	0.26 [42]	
Finishing layer	Gyp.	12.5	660	0.11 [44]	0.09 [44]	
	Memb.	0.6	-	0.15 (decl.)		
	OSBa	14.9	552	1.83 (decl.)	1.13 (decl.)	Less permeable materials
	OSBb	11.8	675	0.59 (decl.)	0.19 (decl.)	
	HCB	18.9	1880	0.34 [45]	0.31 [45]	

Table 1: Thickness, dry density, and order of magnitude of Sd-value of tested materials.

2.2 Methods

Water vapor permeability was measured using the dry and wet cup method following as closely as possible the recommendation of ISO 12572 [11]. Prior to testing, the samples were dried at the temperatures defined in ISO 12570 and then conditioned at 23 °C and 50 %RH. They were then sealed with vapor-tight aluminum tape in PE cups (with dimensions 100 x 100 x 60 mm) containing a desiccant or a saturated salt solution. The sealing efficiency was checked by testing impermeable PVC samples. Three desiccants were tested for the dry cup tests (Silica Gel, Calcium Chloride $CaCl_2$ powder and saturated solution of Potassium Hydroxide KOH), while a saturated solution of Potassium Nitrate KNO_3 was used for wet cup test. Whatever the desiccant, the thickness of air layer between specimen and desiccant was approximately 17 ± 3 mm thick. Temperature and relative humidity in this air layer were monitored at 15 min intervals with small and wireless HygroPuce sensors (Waranet, Auch, France) with an accuracy of 2 %RH and 0.5 °C. The sensors (with dimension 6 mm thick and 16 mm in diameter) were placed either on the surface of the desiccant (Silica Gel) or on a holder above the surface of the desiccant ($CaCl_2$ and KOH). In both cases, the distance d_a between sensor and the undersurface of the sample was evaluated to assess the resistance of the air layer between the sample and the sensor. Figure 1 is schematic view of the experimental set-up.

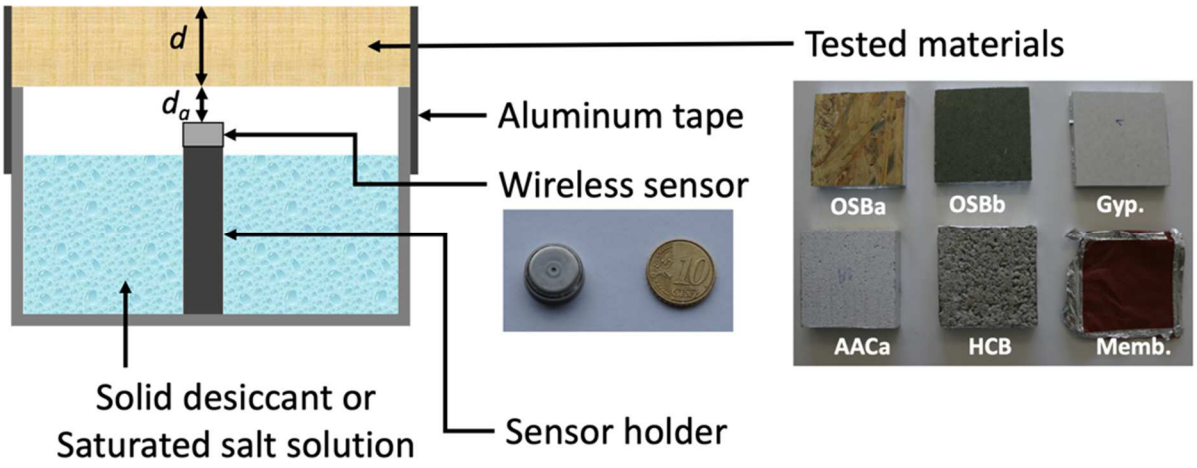

Figure 1: Schematic view of the experimental set-up.

The assemblies were placed in a climatic chamber (Memmert HPP 108, Schwabach, Germany) at 23 °C and 50 %RH. Air velocity measured at 2 cm above the cup with a hot-wire anemometer was 0.15 ± 0.05 $m \cdot s^{-1}$, which is lower than the value recommended for the measurement of highly permeable materials. During experiment, the cups were removed once a day during the working week from the chamber to be weighed using a balance with a precision of 0.01 g (Adventurer Pro AV4102C, Ohaus Corporation, Pine Brook, NJ, USA). This weighing frequency and balance precision are sufficient to obtain results with an accuracy of 5 % according to the Appendix I of ISO 12572 [11] for highly permeable materials. For less permeable materials, one out of two mass points is used in the analysis to reach the required accuracy. The measurements continue until the density of the water vapor flow rate *g* reaches steady state (as specified in section 8.1 of ISO 12572 [11]) or until the assembly has gained more than 1.5 g per 25 ml of desiccant in the cup. With this set-up, this corresponds to a mass gain of about 2.5 $kg \cdot m^{-2}$. In the present study, experiments were run for at least 15 days.

3 Results and discussion

For dry cup experiments, at least five specimens of WFI were tested according to the recommendation of ISO 12572 [11]. The number of specimens of other materials tested ranged between one and three, depending on sensor availability. However, the main objective of this paper is to highlight the influence of boundary conditions inside the cup on the determination of Sd-values, and, whenever possible, this influence is discussed with respect to measurement repeatability, see Appendix A for the repeatability of some measurements. In contrast, instrumented wet cup experiments were performed on only one sample of each material.

3.1 Results obtained with Silica Gel as desiccant

3.1.1 Observation

A first set of experiments was performed using Silica Gel as desiccant. Figures 2a and 2b show variations in relative humidity in the air layer with highly permeable materials (e.g. Sd < 0.3 m) and with less permeable materials (e.g. Sd > 0.3 m), respectively. Temperature variations are plotted in Figures 2c and 2d. Figures 2e and 2f show the density of the water vapor flow rate *g* calculated after each weighing of the samples. For the sake of clarity, only one curve is plotted for each type of material.

Before the start of the experiment, it was verified that relative humidity was 0 %RH and temperature was 23 °C inside the air layer of a cup sealed with impermeable material. At the beginning of the experiment (*i.e.*, just after sealing the sample in the cup), relative humidity in the air layer was 4.5 %RH for low hygroscopic materials (Memb. and HCB) and ranged between 10 %RH and 19 %RH for more hygroscopic materials. These measured relative humidity values differ from the theoretical value of 0 %RH, meaning that moisture supplied by exterior air during cup assembly and by the sample is not instantaneously and totally adsorbed by the desiccant in the early stages. At the same time, the temperature can increase by 3 °C due to moisture adsorption by the desiccant, which is an exothermal reaction.

As the experiment proceeds, moisture flows through the sample due to water vapor pressure gradient. Moisture is adsorbed by the desiccant and the mass of the cup increases. However, the desiccant adsorption capacity decreases gradually over time and relative humidity in the air layer tends to increase. The more permeable material, the bigger the increase in relative humidity. Similar observations were reported by Pazera and Salonvaara [35] in a 24h experiment. After 15 days, the increase in relative humidity ranged from 12 %RH to 22 %RH for highly permeable materials (e.g. Sd < 0.3 m), whereas it did not exceed 6 %RH for less permeable materials (e.g. Sd > 0.3 m). Finally, it could lead to up to 40 %RH

relative humidity measured in the air layer at the end of the experiment. Simultaneously, temperature decreased over a period of 10 days for WFI and Gyp. (because of high moisture adsorption by the desiccant), while equilibrium temperature was reached in less than one day for other materials.

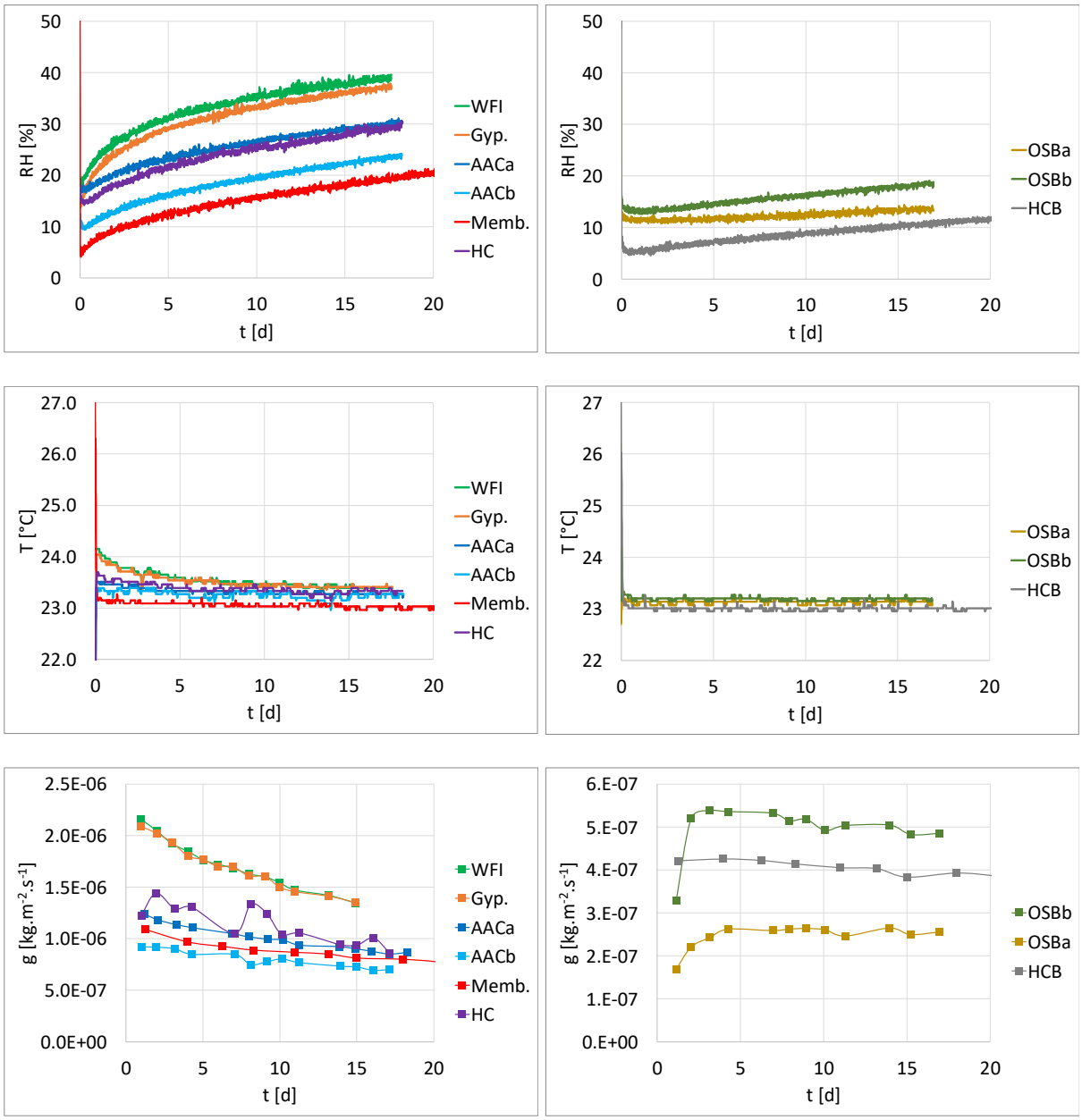

Figure 2: Measured variations in relative humidity and temperature in the air layer and in the density of the water vapor flow rate *g* for highly permeable materials (a,c,e) and less permeable materials (b,d,f) during dry cup experiments performed with Silica Gel.

Because the water vapor pressure gradient decreases across the sample, the density of the water vapor flow rate *g* decreases over time (see Figure 2e and 2f). The decrease is almost negligible with less permeable materials (e.g. Sd > 0.3 m), whereas a reduction up to 50 % is observed with highly permeable materials (e.g. Sd < 0.3 m). Consequently, in the present experiment, steady state (as defined in ISO 12572 [11]) was hard to reach with all highly permeable materials. Particularly with Gyp., Memb. and HC., the last five successive determinations of *g* were within ± 6 % of the mean value of *g* (instead of ± 5% as defined in ISO 12572 [11]). Note that during the experiments none of the samples reached the maximum mass gain of 2.5 kg·m^{-2}.

3.1.2 Data analysis

Once the density of the water vapor flow rate *g* reached steady state, the data were analyzed to evaluate Sd-value by considering the additional resistance of air layers inside and above the cup (as specified in the Appendix G of ISO 12572 [11]):

$$Sd = \mu d = \delta_a \left(\frac{\Delta p_v}{g} - \frac{d_a}{\delta_a} - \frac{1}{h_m} \right) \quad (1)$$

where μ is the water vapor diffusion resistance factor (defined as $\mu = \delta_a / \delta$), δ_a the water vapor permeability of air (equal to $1.95 \cdot 10^{-10}$ kg·m^{-1}·s^{-1}·Pa^{-1} at 23 °C and p_{atm}), δ the material water vapor permeability, *d* the material thickness, Δp_v water vapor pressure difference across the sample, *g* the density of the water vapor flow rate, d_a the thickness of the air layer, and h_m the convective mass transfer coefficient above the cup. The Sd-value was calculated using three approaches:

- In the first approach (noted *th.*), the relative humidity in the air layer is set to a theoretical value of 0 %RH (leading to $\Delta p_v = 1404\ Pa$) and d_a is the distance between undersurface of the sample and the desiccant.
- In the second approach (noted *meas.*), the mean relative humidity measured during the period of analysis is used to calculate Δp_v and d_a corresponds to the distance between undersurface of the sample and the sensor.
- In the third approach (noted *pv*), permeance W (defined as $W = g/\Delta p_v$) is evaluated directly from the measurement. Indeed, Figure 3 shows a linear relationship between the density of the water vapor flow rate g and the difference in the water vapor pressure measured across the sample Δp_v (the correlation coefficient R^2 being higher than 0.97). Therefore, the slope of the curve corresponds to the permeance W. Note, however, that this approach is mainly for highly permeable materials, with which relative humidity in the air layer varies significantly during the experiment.

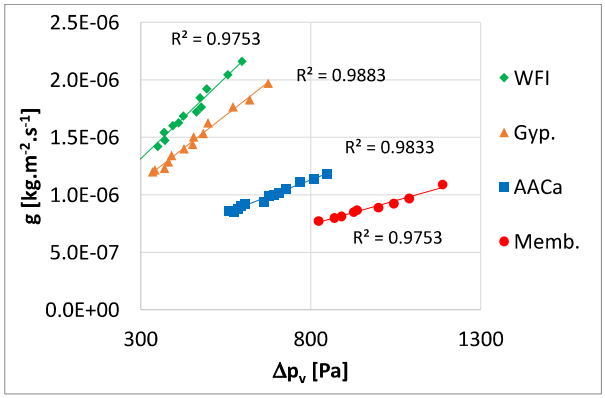

Figure 3: Density of the water vapor flow rate g plotted as function of the difference in the water vapor pressure measured across the sample Δp_v for highly permeable materials.

For the approaches *meas.* and *pv*, a further calculation (noted *RH* in parentheses) is done by modifying the measured relative humidity by 2 %RH (e.g. sensor accuracy). This makes it

possible to evaluate the uncertainty due to sensor precision. Finally, h_m is set to $2.85 \cdot 10^{-8}$ kg·m^{-2}·s^{-1}·Pa^{-1} by default (corresponding to an external resistance of $3.5 \cdot 10^{7}$ m^2·s·Pa·kg^{-1}). This value was measured during water evaporation experiments [46] and is similar to data reported in the literature [36,46-47]. Nevertheless, with a view to evaluating the sensitivity of Sd-value to moisture transfer resistance, an alternative value of $1 \cdot 10^{-8}$ kg·m^{-2}·s^{-1}·Pa^{-1} was used for h_m (noted *hm* in parentheses). In addition, internal and external resistance is discussed in Appendix B.

The Sd-values calculated using these approaches are plotted in Figures 4a and 4b for highly and less permeable materials, respectively. When calculated in the same way as in ISO 12572 (approach *th.*), $Sd_{th.}$ differed significantly from the declared or literature data (see Table 1). The differences ranged between -44 % (for OSBa) and 100 % (for Memb.). They are higher than measurement uncertainty (which ranged from 7 % (for HCB) to 27 % (for WFI)) and than sensitivity to h_m (which was less than 10 %). In our opinion, the period of analyis and the adsorption capacity of the dessicant are extremely important when calculating Sd-value using the *th.* approach. When using measured relative humidity in the analysis (approach *meas.*), the measurement uncertainty is reduced to maximum 14 % and $Sd_{meas.}$ is obviously lower because of lower Δp_v . The relative difference (defined as $(Sd_{th.} - Sd_{meas.})/Sd_{meas.}$) ranged between 20 % and 450 % and decreased with an increase in the Sd-value. In comparison, sensitivity to h_m was limited: relative differences were of about 60 % for WFI and Gyp., but less than 13 % for materials with $Sd_{meas.} > 0.1\,m$. Similarly, sensitivity to *RH* was also limited: relative differences were highest for highly permeable materials (because of low Δp_v) but did not exceed 30 %. For all the materials tested, the sensitivity to h_m and to *RH* was at least 3 times lower than the influence of the relative humidity of the air layer (*meas.* vs *th.*). Nevertheless, using measured relative

humidity can lead to lower $Sd_{meas.}$ than sample thickness (e.g. $\mu < 1$) for highly permeable materials like WFI. It should mean that water vapor diffusion is faster inside the material than in the air, which is unrealistic. This is not the case when permeance W is evaluated directly from the measurement (approach pv) in which case Sd_{pv} is higher than $Sd_{meas.}$ (with a relative difference ranging between 11 % and 63 %). With approach pv, measurement uncertainty and sensitivity to RH are still limited, unlike sensitivity to h_m. The pv approach thus seems to be an appropriate method to evaluate a realistic Sd-value for very highly permeable materials (e.g. $Sd < 0.1\,m$). Lastly, absolute differences between the three approaches ranged between 0.1 m and 0.25 m, *i.e.* the difference are significant.

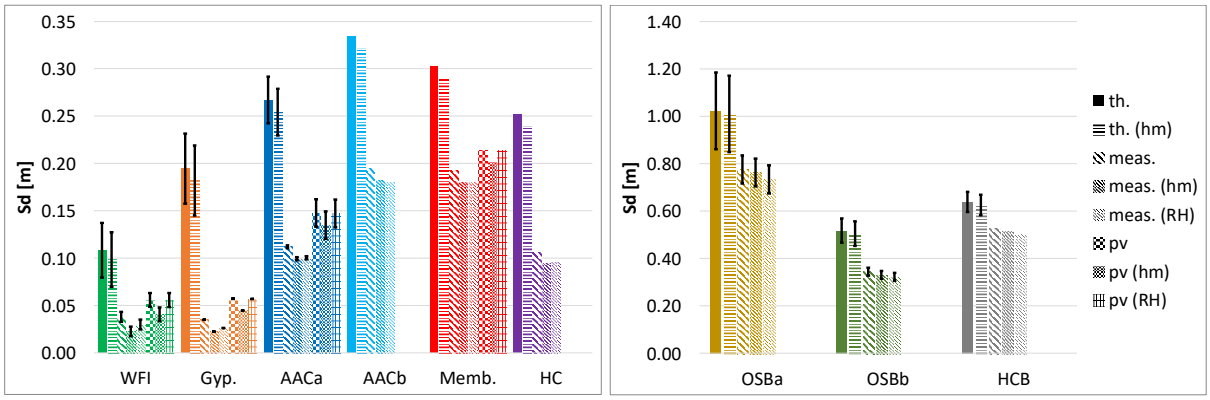

Figure 4: Sd-values calculated from dry cup experiments with Silica Gel using theoretical (*th.*), measured (*meas.*) relative humidity or measured permeance (*pv*) for two levels of convective mass transfer coefficient h_m for highly permeable (a) and less permeable (b) materials.

3.2 Influence of desiccant in the dry cup experiment

Further experiments were performed using $CaCl_2$ and KOH as desiccant. In particular, special attention has to be paid when experiments are conducted using KOH saturated solution. The cups have to be handled very carefully to avoid wetting the sensor and the

sample. Therefore, initial air layer thickness was closed to 20 mm for these experiments. During the experiment, vapor uptake by the cup increase the level of the solution (by reducing the thickness of the air layer): the maximal increase was up to 3 mm in the case of the most permeable materials. It was checked that this air layer thickness decrease (or increase of volume or mass of the solution) is consistent with the mass change of the cups between the beginning and the end of the experiment. Lastly, it was checked that the solution was still saturated at the end of the experiment. Concerning $CaCl_2$, only a 2-mm thick rigid layer was observed at the upper surface of the desiccant at the end of experiment.

Figures 5a and 5b compare variations in measured relative humidity in the air layer with the three desiccants for gypsum board (highly permeable material) and hollow concrete blocks (less permeable material). Figures 5c and 5d compare variations in temperature. Using $CaCl_2$, relative humidity again differed from 0 %RH in the early stage and then increased over time, similar to Silica Gel. Since the sorption capacity of $CaCl_2$ is higher than that of one of Silica Gel [48], the increase was smaller for highly permeable materials. However, temperature decreased more slowly due to higher sorption heat and had not reached thermal equilibrium after 20 days.

In case of less permeable materials, with Silica Gel, differences in relative humidity and temperature were negligible. The density of the water vapor flow rate g decreased only slightly compared to that of Silica Gel, and steady state was reached even for the most permeable materials.

With KOH, temperature and relative humidity were constant after one day. However, measured relative humidity values ranged between 20 %RH and 30 %RH for highly permeable materials and around 14 %RH for less permeable materials. These values differed from the theoretical value (8.5 %RH) predicted under thermodynamic equilibrium. There are two possible explanations for these differences. First, the measurement was not taken exactly

at the interface between the air and the saturated solution. Second, a saturated salt solution is in fact not under thermodynamic equilibrium. However, to the best of our knowledge, saturated salt solutions have been rarely investigated under non-equilibrium conditions. Whatever the material, steady state could be easily reached when using KOH solutions.

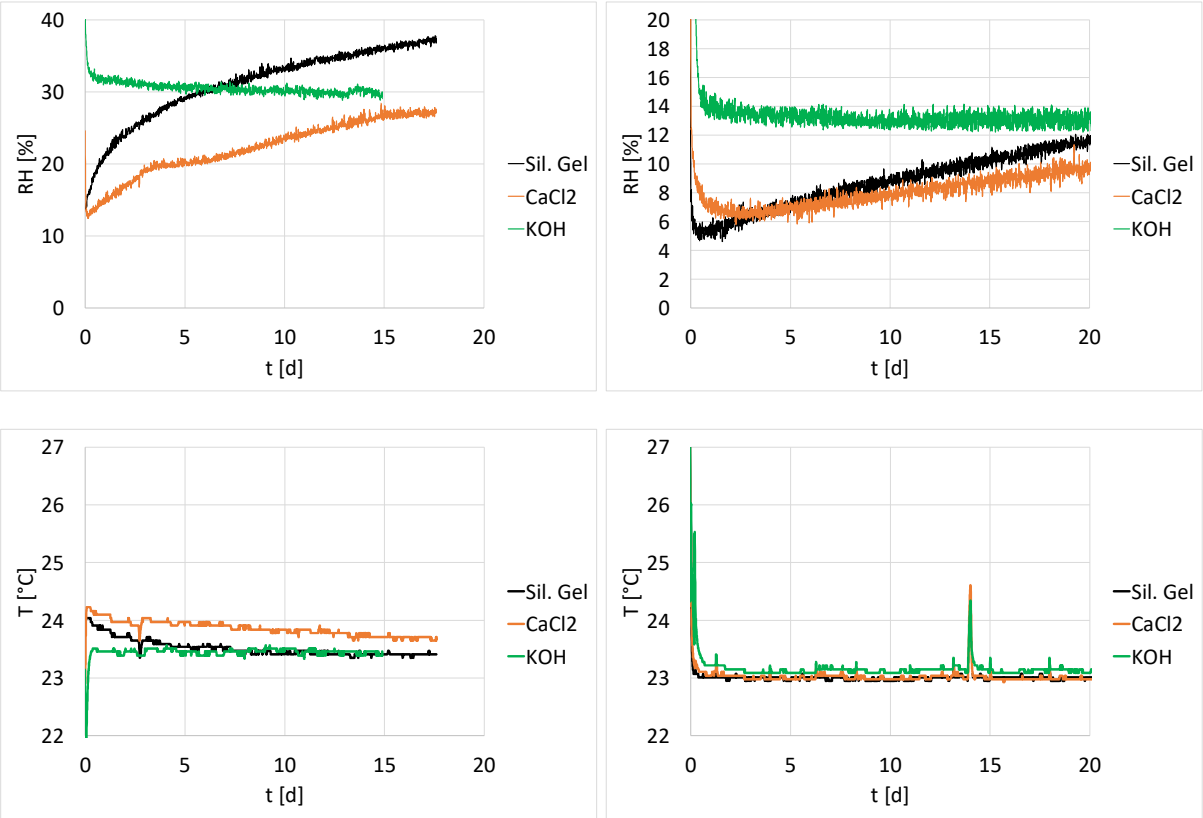

Figure 5: Measured variations in relative humidity and in temperature in the air layer with different desiccants for gypsum board (highly permeable material) (a) and for hollow concrete blocks (less permeable material) (b).

Figures 6a and 6b show the calculated Sd-value of both materials with the three desiccants using approaches *th.* and *meas.*. As shown in Figure 4, sensitivity to h_m and *RH* was also evaluated. $Sd_{th.}$ is dependent on the desiccant (particularly in the case of highly permeable materials). For Gyp., the highest measurement uncertainty was observed with Silica Gel, whereas repeatability was better with $CaCl_2$ and KOH. Particularly with $CaCl_2$, $Sd_{th.}$ was very close to data reported in the literature using the same desiccant [44], the slight

difference being due to sensitivity to h_m. As was the case for measurements performed with Silica Gel, $Sd_{meas.}$ was lower than $Sd_{th.}$ whatever the desiccant. Differences between $Sd_{th.}$ and $Sd_{meas.}$ ranged between 15 % and 150 % with $CaCl_2$ and between 3 % and 110 % with KOH for all the materials tested. By comparison, sensitivity to h_m and to RH was at least 2 times lower than the influence of the relative humidity of the air layer (*meas.* vs *th.*). Finally, fewer differences in $Sd_{meas.}$ were observed between desiccants.

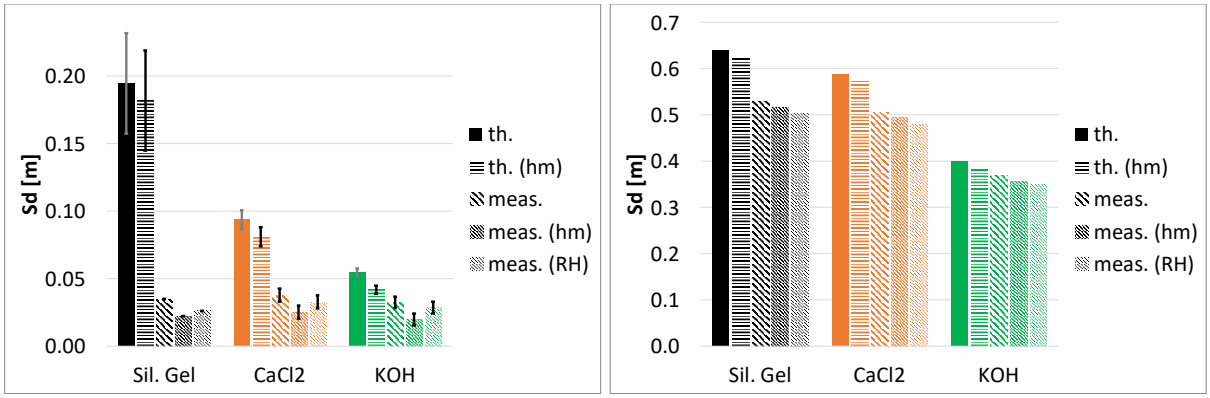

Figure 6: Sd-values calculated using different desiccant for gypsum board (highly permeable material) (a) and for hollow concrete blocks (less permeable material) (b).

Figures 7a and 7b show the relative differences between $Sd_{meas.}$ and Sd_{th} measured for all the materials with the three desiccants as function of $Sd_{meas.}$ and of $RH_{air\ layer} - RH_{th}$ respectively. With Silica Gel, the relative differences were greater than 35 % for $Sd_{meas.} < 0.35\ m$. This is due to the high relative humidity in the air layer caused by the low adsorption capacity of Silica Gel. With $CaCl_2$ and KOH (that both have a higher adsorption capacity than Silica Gel), the relative differences were less than 30 % for $Sd_{meas.} > 0.1\ m$. With the three desiccants, the relative difference decreased according to a power law (the correlation coefficient R^2 being higher than 0.85):

$$\frac{Sd_{th.} - Sd_{meas.}}{Sd_{meas.}} = A(Sd_{meas.})^{-B} \quad (2)$$

where A and B are fitting parameters.

Figure 7b shows that the relative differences were clearly related to the difference between measured relative humidity in the air layer $RH_{air\ layer}$ and the theoretical value RH_{th} as shown by the exponential relationship (the correlation coefficient R^2 being higher than 0.99):

$$\frac{Sd_{th.}-Sd_{meas.}}{Sd_{meas.}} = C\ exp\left(D\left(RH_{air\ layer} - RH_{th}\right)\right) \quad (3)$$

where C and D are fitting parameters.

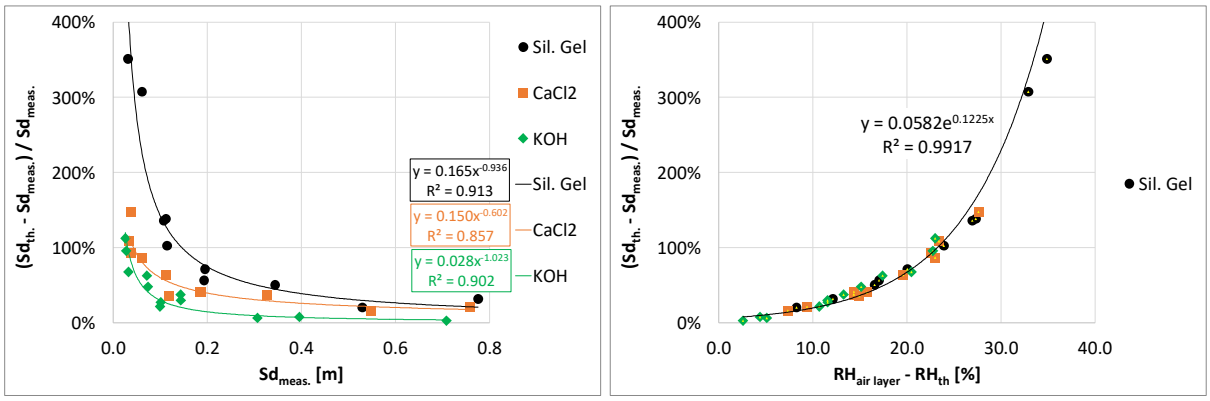

Figure 7: Relative differences between $Sd_{meas.}$ and Sd_{th} as function of $Sd_{meas.}$ (a) and of $RH_{air\ layer} - RH_{th}$ (b) with the three desiccants and for all materials.

For Silica Gel and KOH, we particularly note that exponent B is closed to one. In this case, equation (2) becomes:

$$Sd_{meas.} \overset{B\approx 1}{\Longrightarrow} Sd_{th.} - A \quad (4)$$

In practice, this result means that experiments can be carried out as usual following ISO 12572 [11] and analyzed assuming theoretical values of relative humidity in the air layer (0% RH for Silica Gel and 8.5 %RH for KOH). The calculated Sd-value $Sd_{th.}$ can then be easily corrected by factor A to assess the real Sd-value $Sd_{meas.}$. Here, the correction factor used was 0.165 m for Silica Gel and 0.028 m for KOH. Incidentally, the real relative humidity in the air layer and hence the mean relative humidity within the sample, can be evaluated as:

$$RH_{air\ layer} \overset{B\approx 1}{\Longrightarrow} RH_{th} + \frac{1}{D}\ln\left(\frac{A}{C(Sd_{th.}+A)}\right) \quad (5)$$

The fitting factors used in Equations (4) and (5) prevail for the current experiments (cup design, outer boundary conditions) and could thus be used to estimate real $Sd_{meas.}$ and $RH_{air\ layer}$ in experimental set-up similar to ours.

3.3 Wet cup experiment

Wet cup experiments were performed once on the same materials, paying particular attention to avoid wetting the sensor and the sample. For these experiments, air layer is initially set to 15 mm and it increases over time. Figures 8a and 8b show variations in the relative humidity of the air layer for highly permeable materials and for less permeable materials (except for HCB), respectively. After a few days, the $RH_{air\ layer}$ of all the materials was almost constant. A theoretical value of 93 %RH was reached for the less permeable materials. the measured relative humidity of highly permeable materials was less than 93 %RH, the biggest difference being observed for the most permeable materials. These observations are in line with the ones made with KOH, confirming that assessing the behavior of saturated salt under non-equilibrium conditions is a key point.

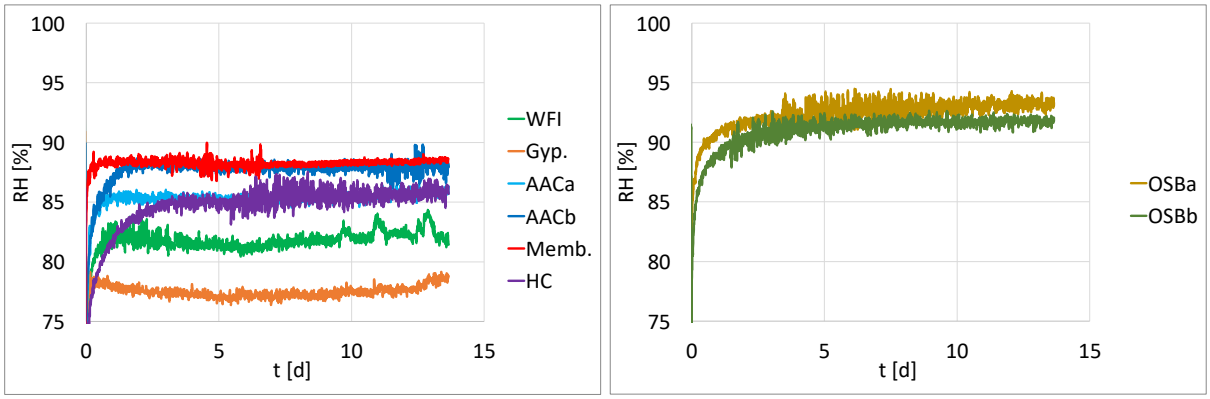

Figure 8: Measured variations in relative humidity in the air layer for highly permeable materials (a) and less permeable materials (b) during wet cup experiments.

Figures 9a and 9b presents the calculated Sd-values using approaches *th.* and *meas.* for highly and less permeable materials, respectively. $Sd_{th.}$ and $Sd_{meas.}$ calculated for dry cup experiments with Silica Gel are also plotted for the sake of comparison. Similarly to the results presented in Figure 4, using measured relative humidity in the analysis led to lower Sd-values since there was less difference in water vapor pressure across the sample Δp_v. Nevertheless, the relative differences between the two approaches were lower (they did not exceed 80 %) and also decreased with increasing measured Sd-value, as shown in Figure 6a. In this case, the coefficients of equation (2) are A = 0.0168 and B = 1.106 (the correlation coefficient R^2 being higher than 0.91). These relative differences are also related to the difference $RH_{air\ layer} - RH_{th}$ between relative humidity measured in the air layer and the theoretical value. The results obtained in the wet cup experiment perfectly match with the trend in Figure 7b. Since B is close to 1, the approximation proposed in equations (4) and (5) also prevails for wet cup experiments.

When we compared dry and wet cup experiments, we observed that $Sd^{dry} > Sd^{wet}$ when the theoretical relative humidity value was used for the air layer. This observation is in line with observations reported in the literature (see Table 1). When we used measured relative humidity in the analysis, $Sd^{dry} > Sd^{wet}$ only for Memb.. For all the other materials (except HCB), $Sd^{dry} \approx Sd^{wet}$ considering measurement uncertainties. Such a results is not necessarily surprising. Indeed, mean relative humidity of the materials varied between 31 %RH and 43 %RH in the dry cup experiments and between 64 %RH and 75 %RH in the wet cup

experiments. Between these relative humidity values, the moisture content of the material increases but only to a small extent in the hygroscopic domain. Therefore, the reduction in the diffusion area and the increase in the tortuous diffusion path should be very limited. Consequently, only small differences between dry and wet cup experiments are expected.

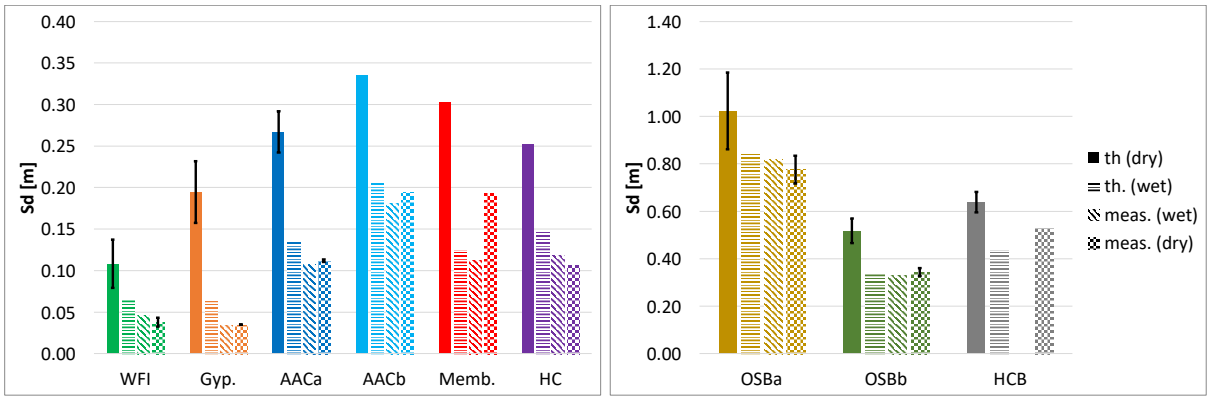

Figure 9: Sd-values calculated from wet cup experiments using theoretical (th.) and measured (meas.) relative humidity for highly permeable materials (a) and less permeable materials (b).

4 Conclusions

Dry and wet cup experiments were performed using different solid desiccants or saturated salt solutions on nine materials with Sd-values ranging between 0.08 m and more than 1 m. In all the experiments, a wireless sensor was placed inside the air layer to monitor temperature and relative humidity. At the beginning of the experiment, it was observed that the measurements differed from the expected theoretical values whatever the permeability of the materials. During the experiments, solid desiccants saturated progressively, the relative humidity within the air layer and hence the density of the water vapor flow rate varied over time. In particular, with Silica Gel, steady state could even not be reached for the most permeable materials tested. On the other hand, saturated salt solutions provided more stable conditions in the air layer. Sd-values were calculated using two methods with measured relative humidity and compared to theoretical values. Differences were observed between $Sd_{th.}$ and $Sd_{meas.}$. These differences were larger than the measurement uncertainty and also than the sensitivity to external air resistance and to sensor precision Whatever the desiccant, the relative difference increased with decreasing measured Sd-values according to a power law and were clearly linked to differences between the measured and the theoretical relative humidity in the air layer. When the power exponent is close to one, a methodology is proposed to evaluate the “real” Sd-value from the theoretical Sd-value. We suggested that this methodology can be used in experiments like ours to correct the measured water vapor permeability. Finally, we observed almost no differences between the dry and wet cup experiments when we used measured relative humidity for the analysis whereas we noted the usual differences when we used the theoretical relative humidity for the analysis.

5 Nomenclature

Latin characters

d	m	Material thickness
da	m	Air layer thickness
g	$kg \cdot m^{-2} \cdot s^{-1}$	Density of the water vapor flow rate
hm	$kg \cdot m^{-2} \cdot s^{-1} \cdot Pa^{-1}$	Convective mass transfer coefficient
RH	%	Relative humidity
Sd	m	Sd-value
T	°C	Temperature
W	$kg \cdot m^{-2} \cdot s^{-1} \cdot Pa^{-1}$	Material permeance
Z	$m^2 \cdot s \cdot Pa \cdot kg^{-1}$	Material resistance

Greek characters

δ	$kg \cdot m^{-1} \cdot s^{-1} \cdot Pa^{-1}$	Material water vapor permeability
δ_a	$kg \cdot m^{-1} \cdot s^{-1} \cdot Pa^{-1}$	Water vapor permeability of air
Δp_v	Pa	Water vapor pressure difference across the sample.
μ	-	Water vapor diffusion resistance factor
ρ	$kg \cdot m^{-3}$	Material density

Indices

meas.	measured
th.	theoretical

6 Appendix A: discussion about repeatability

Dry cup experiments with Silica Gel as desiccant were performed on six specimens of WFI. Figures A1a and A1b show variations in the relative humidity in the air layer and in the density of the water vapor flow rate *g* recorded in all experiments. Two groups of experiments can be distinguished. Specimens 1 and 6 had higher relative humidity and lower *g* than the other specimens. The Silica Gel used for these two specimens was less dry and its adsorption capacity was consequently lower. Nevertheless, the kinetic were very similar whatever the specimens.

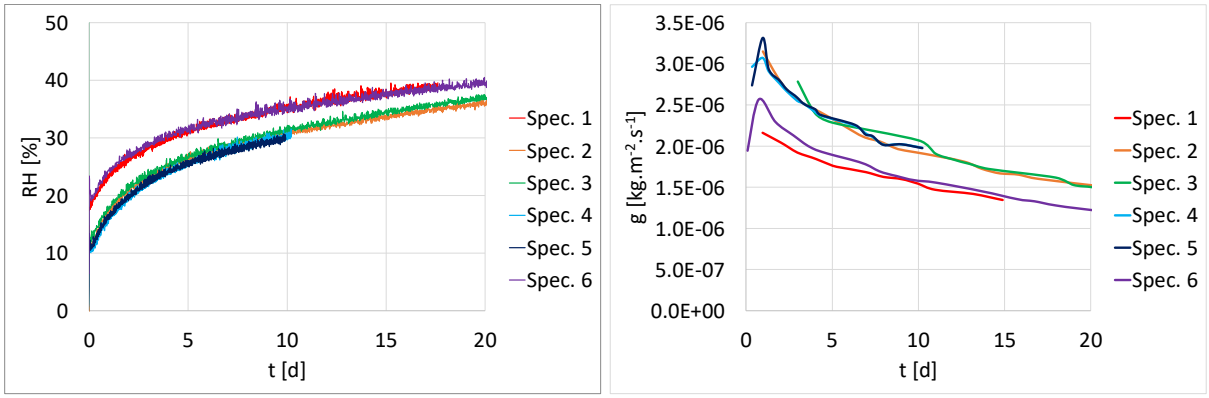

Figure A1: Variations in measured relative humidity in the air layer (a) and in the density of the water vapor flow rate *g* (b) during dry cup experiments performed on specimens of WFI using Silica Gel.

Figure A2 shows the calculated Sd-value for each specimens following the methodology described in Section 3.1.2. Marked differences can be seen in the theoretical calculation (assuming 0 %RH in the air layer). These differences are due to differences in the period of analysis of the data. For specimens 4 and 5, steady state is reached in less than 5 days, while it took more than 10 days for other specimens. The density of the water vapor flow rate *g* is therefore higher and the Sd-value is lower. This leads to high uncertainty. When measured

values in the air layer are used in the analysis (meas. or pv), there is less difference between specimens and uncertainty is reduced. Similar observations were made for other materials tested with Silica Gel.

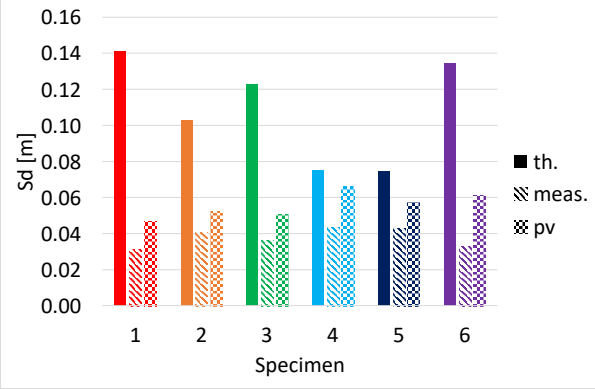

Figure A2: Sd-values calculated from dry cup experiments on WFI specimens with Silica Gel using theoretical (*th.*), measured (*meas.*) relative humidity or measured permeance (*pv*).

Further dry cup experiments were performed with $CaCl_2$ and KOH. The results obtained on a few Gyp. specimens are plotted in Figures A3 and A4. Good repeatability of the experimental data was observed whatever the desiccant. Consequently, the differences in Sd-value were very limited with both calculation approaches. Finally, good reliability of the results can be expected with both desiccants.

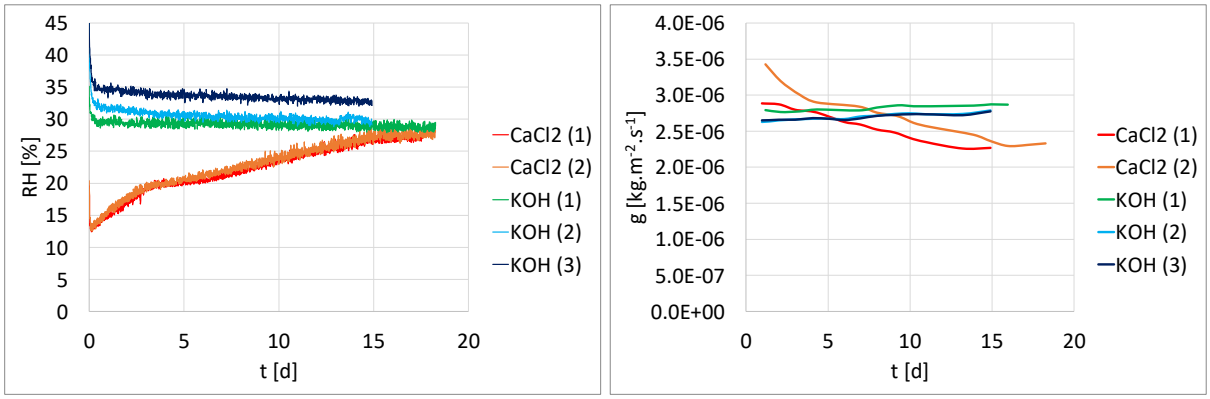

Figure A3: Measured variations in relative humidity in the air layer (a) and in the density of the water vapor flow rate *g* (b) during dry cup experiments performed on Gyp specimens with $CaCl_2$ and KOH.

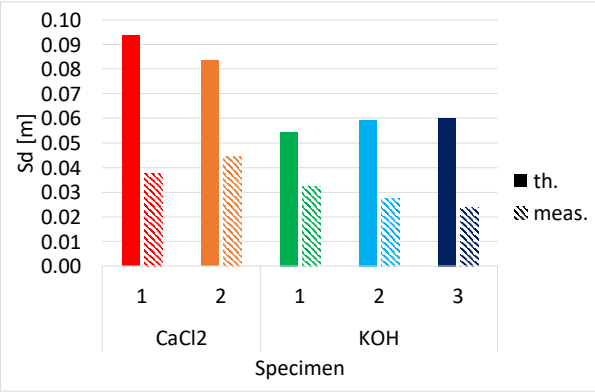

Figure A4: Sd-values calculated from dry cup experiments on Gyp. specimens with $CaCl_2$ and KOH using theoretical (*th.*) and measured (*meas.*) relative humidity.

7 Appendix B: discussion about air resistances

Dry cup experiments with Silica Gel as desiccant were performed for different thicknesses of WFI (d = 40 mm or $2d$ = 80 mm) and different air layer thicknesses (d_a = 10 mm or 2 d_a = 20 mm), inspired by the Appendix H of ISO 12572 [11]. Figure B1 shows variations in relative humidity in the air layer observed in all the experiments. These variations are obviously sensitive to the thickness of the material, while the thickness of the air layer has only a minor influence. Indeed, increasing the thickness of the material decreases the density of the water vapor flow rate g and the desiccant consequently saturates more slowly.

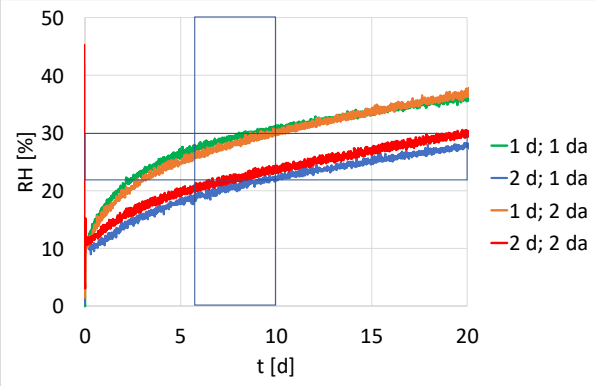

Figure B1: Influence of the thickness d of the material and of the thickness da of the air layer on measured variations in relative humidity in the air layer during dry cup experiments performed on WFI using Silica Gel.

Resistance can be evaluated for each experiment. Let Z_{xy} denote the resistance measured for a sample with a thickness of x times d and for an air layer with a thickness of y times d_a. This resistance is the sum of the external air resistance Z_{ext}, of x times the material resistance Z_{mat} and of y times the internal air resistance Z_{int}. Therefore, Z_{int} and Z_{ext} can be calculated as:

$$Z_{int} = Z_{12} - Z_{11} \quad \text{(A1)}$$

$$Z_{ext} = 2Z_{11} - Z_{22} \quad \text{(A2)}$$

Note that Appendix H of ISO 12572 [11] recommends evaluating $2Z_{11} - Z_{21}$, which is in fact the sum of Z_{int} and Z_{ext}. The resistance can be evaluated from experimental data in two ways: either at the same time (green aera in Figure B1) or for the same relative humidity in the air layer (blue area in Figure B1). Further, resistance can be calculated from the mean value of the density of the water vapor flow rate *g* or from the permeance *W* evaluated as in Figure 2. Table B1 summarized all the above-mentioned results and also gives the theoretical values for the purpose of comparison. Regarding Z_{int}, agreement is good despite the difficulty of accurately measuring the thickness of the air layer in the presence of Silica Gel packed beads. However, the method proposed in Appendix H generally leads to higher resistance, which depends on the evaluation procedure. Therefore, we suggest not following the Appendix H, but instead estimating Z_{int} theoretically. Regarding Z_{ext}, the values are slightly higher than the value measured during water evaporation experiments since surface rugosity can limit the vapor transfer. Nevertheless, the observed differences have a limited influence on measured Sd-value compared to the level of relative humidity in the air layer.

		Same time		Same RH	
	Theoretical	Mean *g*	*W*	Mean *g*	*W*
Z_{int} Eq. (A1)	$5.1 \cdot 10^7$	$4.14 \cdot 10^7$	$6.45 \cdot 10^7$	$4.21 \cdot 10^7$	$5.69 \cdot 10^7$
Z_{ext} Eq. (A2)	$3.5 \cdot 10^7$	$3.63 \cdot 10^7$	$4.19 \cdot 10^7$	$6.24 \cdot 10^7$	$1.10 \cdot 10^8$
$Z_{int} + Z_{ext}$ (Annex H)		$3.87 \cdot 10^7$	$7.56 \cdot 10^7$	$6.33 \cdot 10^7$	$1.18 \cdot 10^8$

Table B1: Measured surface resistance according to the different approaches.

8 References

[1] NF DTU 31.2 (2019). Building works - Timber frame houses and buildings construction - Part 1-1 : Contract bill of technical model clauses.

[2] ISO 13788 (2012). Hygrothermal performance of building components and building elements - Internal surface temperature to avoid critical surface humidity and interstitial condensation - Calculation methods.

[3] Cascione, V., Marra, E., Zirkelbach, D., Liuzzi, S., & Stefanizzi, P. (2017). Hygrothermal analysis of technical solutions for insulating the opaque building envelope. Energy Procedia, 126, 203-210.

[4] Zhou, X., Carmeliet, J., & Derome, D. (2018). Influence of envelope properties on interior insulation solutions for masonry walls. Building and Environment, 135, 246-256.

[5] Vereecken, E., & Roels, S. (2016). Capillary active interior insulation systems for wall retrofitting: a more nuanced story. International Journal of Architectural Heritage, 10(5), 558-569.

[6] Zhao, J., Plagge, R., Nicolai, A., Grunewald, J., & Zhang, J. S. (2011). Stochastic study of hygrothermal performance of a wall assembly—The influence of material properties and boundary coefficients. HVAC&R Research, 17(4), 591-601.

[7] ISO 11092 (2014). Textiles -- Physiological effects -- Measurement of thermal and water-vapour resistance under steady-state conditions (sweating guarded-hotplate test).

[8] ASTM F 2298 (2009). Standard Test Methods for Water Vapor Diffusion Resistance and Air Flow Resistance of Clothing Materials Using the Dynamic Moisture Permeation Cell.

[9] Challansonnex, A., Pierre, F., Casalinho, J., Lv, P., & Perre, P. (2018). Mass diffusivity determination of various building materials based on inverse analysis of relative humidity evolution at the back face of a sample. Construction and Building Materials, 193, 539-546.

[10] Busser, T., Berger, J., Piot, A., Pailha, M., & Woloszyn, M. (2018). Dynamic experimental method for identification of hygric parameters of a hygroscopic material. Building and Environment, 131, 197-209.

[11] ISO 12572 (2016). Hygrothermal performance of building materials and products - Determination of water vapour transmission properties - Cup method.

[12] EN 12086 (2013). Thermal insulating products for building applications - Determination of water vapour transmission properties.

[13] ASTM E96 (2016). Standard test methods for water vapour transmission of materials.

[14] Feng, C., Janssen, H., Feng, Y., & Meng, Q. (2015). Hygric properties of porous building materials: Analysis of measurement repeatability and reproducibility. Building and Environment, 85, 160-172.

[15] Galbraith, G. H., McLean, R. C., Tao, Z., & Kang, N. (1992). The comparability of water vapour permeability measurements: investigation assessing comparability of measured vapour permeability values obtained from range of laboratories throughout European Community. Building Research and Information, 20(6), 364-372.

[16] Time, B., & Uvsløkk, S. (2003). Intercomparison on measurement of water vapour permeance. Nordtest–project agreement 1529-01.

[17] Roels, S., Carmeliet, J., Hens, H., Adan, O., Brocken, H., Cerny, R., Pavlík, Z., Hall, C., Kumaran, K., Pel, L., Plagge, R. (2004). Interlaboratory comparison of hygric properties of porous building materials. Journal of thermal envelope and building science, 27(4), 307-325.

[18] Roels, S., Talukdar, P., James, C., & Simonson, C. J. (2010). Reliability of material data measurements for hygroscopic buffering. International Journal of Heat and Mass Transfer, 53(23-24), 5355-5363.

[19] Feng, C., Guimarães, A. S., Ramos, N., Sun, L., Gawin, D., Konca, P., ... & Janssen, H. (2020). Hygric properties of porous building materials (VI): A round robin campaign. Building and Environment, 185, 107242.

[20] Bomberg, M. (1989). Testing water vapor transmission: Unresolved issues, In Water Vapor Transmission Through Building Materials and Systems: Mechanisms and Measurement. ASTM International.

[21] Mukhopadhyaya, P., Kumaran, K., Lackey, J., van Reenen, D. (2007). Water Vapor Transmission Measurement and Significance of Corrections, In Heat-Air-Moisture Transport: Measurements on Building Materials. ASTM International.

[22] Manelius, E., & Vinha, J. (2011). The Effect of Leakage through the Sealant in the Cup Test Method, In Proceeding of the 9th Nordic Symposium on Building Physics.

[23] Zelinka, S. L., Glass, S. V., & Boardman, C. R. (2016). Improvements to water vapor transmission and capillary absorption measurements in porous materials. Journal of Testing and Evaluation, 44(6), 2396-2402.

[24] Richter, J., & Staněk, K. (2016). Measurements of water vapour permeability–tightness of fibreglass cups and different sealants and comparison of μ-value of gypsum plaster boards. Procedia Engineering, 151, 277-283.

[25] Vololonirina, O., & Perrin, B. (2016). Inquiries into the measurement of vapour permeability of permeable materials. Construction and Building Materials, 102, 338-348.

[26] Seng, B., Magniont, C., & Lorente, S. (2019). Characterization of a precast hemp concrete block. Part II: Hygric properties. Journal of Building Engineering, 24, 100579.

[27] Talev, G., Jelle, B. P., Næss, E., Gustavsen, A., & Thue, J. V. (2013). Measurement of the convective moisture transfer coefficient from porous building material surfaces applying a wind tunnel method. Journal of Building Physics, 37(1), 103-121.

[28] Mortensen, L. H., Rode, C., & Peuhkuri, R. H. (2005). Effect of airflow velocity on moisture exchange at surfaces, IEA ECBCS Annex 41 Meeting.

[29] Galbraith, G. H., Kelly, D. J., & McLean, R. C. (2004). Moisture permeability measurements under reduced barometric pressures. Materials and Structures, 37(5), 311-317.

[30] Fořt, J., Pavlík, Z., Žumár, J., Pavlíková, M., & Černý, R. (2014). Effect of temperature on water vapor transport properties. Journal of Building Physics, 38(2), 156-169.

[31] Olaoye, T. S., Dewsbury, M., & Künzel, H. (2021). Empirical investigation of the hygrothermal diffusion properties of permeable building membranes subjected to variable relative humidity condition. Energies, 14(13), 4053.

[32] McLean, R. C., Galbraith, G. H., & Sanders, C. H. (1990). Testing building materials: Vapour transmission performance of building materials with particular reference to application of computational techniques for interstitial condensation prediction. Building Research and Practice, 18(2), 82-91.

[33] Iizuka, S., Murata, K., Sekine, M., & Sato, C. (2016). A novel cup with a pressure-adjusting mechanism for high-temperature water vapor transmission rate measurements. Polymer Testing, 50, 73-78.

[34] Liersch, K. W., & Schelisch, J. (2002). Methoden zur Bestimmung der diffusionsäquvalenden Luftschichtdicke von extrem diffusionsoffenen Materialien. Bauphysik, 24(3), 150-156.

[35] Pazera, M., & Salonvaara, M. (2009). Examination of stability of boundary conditions in water vapor transmission tests. Journal of Building Physics, 33(1), 45-64.

[36] McGregor, F., Fabbri, A., Ferreira, J., Simões, T., Faria, P., & Morel, J. C. (2017). Procedure to determine the impact of the surface film resistance on the hygric properties of composite clay/fibre plasters. Materials and Structures, 50(4), 1-13.

[37] Colinart, T., & Glouannec, P. (2020). On the importance of desiccant during the determination of water vapor permeability of permeable insulation material. In E3S Web of Conferences (Vol. 172, p. 14003). EDP Sciences.

[38] Zubarev, K., & Gagarin, V. (2019, December). Determining the coefficient of mineral wool vapor permeability in vertical position. In Energy Management of Municipal Transportation Facilities and Transport (pp. 593-600).

[39] Berger, J., Colinart, T., Loiola, B. R., & Orlande, H. R. (2020). Parameter estimation and model selection for water sorption in a wood fibre material. Wood Science and Technology, 54(6), 1423-1446.

[40] Colinart, T., Bendouma, M., & Glouannec, P. (2019). Building renovation with prefabricated ventilated façade element: A case study. Energy and Buildings, 186, 221-229.

[41] Bendouma, M., Colinart, T., Glouannec, P., & Noël, H. (2020). Laboratory study on hygrothermal behavior of three external thermal insulation systems. Energy and Buildings, 210, 109742.

[42] Lelievre, D., Colinart, T., & Glouannec, P. (2014). Hygrothermal behavior of bio-based building materials including hysteresis effects: Experimental and numerical analyses. Energy and Buildings, 84, 617-627.

[43] Jerman, M., Keppert, M., Výborný, J., & Černý, R. (2013). Hygric, thermal and durability properties of autoclaved aerated concrete. Construction and building materials, 41, 352-359.

[44] Roels, S., & Carmeliet, J. (2005). Water vapour permeability and sorption isotherm of coated gypsum board. In Proceedings of the 7th symposium on building physics.

[45] Delgado, J. M. P. Q., Azevedo, A. C., & Guimarães, A. S. (2019). Influence of hydraulic contact interface on drying process of masonry walls. Drying Technology.

[46] Talev, G., Gustavsen, A., & Næss, E. (2008). Influence of the Velocity, Local Position, and Relative Humidity of Moist Air on the Convective Mass Transfer Coefficient in a Rectangular Tunnel—Theory and Experiments. Journal of Building Physics, 32(2), 155-173.

[47] Kwiatkowski, J. (2009). Moisture in buildings, air-envelope interaction. PhD Thesis. Institut National des Sciences Appliquées de Lyon.

[48] Zhang, H., Yuan, Y., Sun, Q., Cao, X., & Sun, L. (2016). Steady-state equation of water vapor sorption for CaCl 2-based chemical sorbents and its application. Scientific reports, 6(1), 1-8.